Consequences of residual-entropy hierarchy violation for behavior of the specific heat capacity in frustrated magnetic systems: An exact theoretical analysis

E. Jurčišinová and M. Jurčišin

Institute of Experimental Physics, Slovak Academy of Sciences, Watsonova 47, 040 01 Košice, Slovakia
and Bogoliubov Laboratory of Theoretical Physics, Joint Institute for Nuclear Research, 141 980 Dubna, Moscow Region, Russian Federation

(Received 14 November 2018; published 30 April 2019)

We investigate in detail the influence of the violation of the strict residual-entropy hierarchy among the neighboring ground states of different orders on the low-temperature behavior of the specific heat capacity in the magnetic frustrated systems in the framework of the exactly solvable antiferromagnetic spin-1/2 Ising model with the multisite interaction in the presence of the external magnetic field on the zigzag ladder. The exact expressions for the residual entropies of all ground states of the model are found, and it is shown that when the strength of the multisite interaction is strong enough then the model exhibits a quite interesting specific situation, namely, that there exist neighboring plateau ground states together with the single-point ground state that separates them, such that the magnetization properties of all of them are different but their entropy per site is the same and equal to zero. It is shown that this fact of the violation of the strict residual-entropy hierarchy between neighboring ground states of different orders leads to the reduction of the possible number of peaks that can appear in the low-temperature behavior of the specific heat capacity in the corresponding regions of the model parametric space. In addition, it is also shown that the absence of the strict residual-entropy hierarchy among neighboring ground states of different orders changes qualitatively the behavior of the specific heat capacity as a function of the external magnetic field, namely, that the typical field-induced sharp double-peak structure in the low-temperature behavior of the specific heat capacity, which is directly related to the very existence of the highly macroscopically degenerated single-point ground states, disappears already for relatively large values of the temperature.

DOI: 10.1103/PhysRevE.99.042151

I. INTRODUCTION

The existence of various low-temperature anomalies of the specific heat capacity, such as the formation of the two-peak structure (known as the Schottky-type anomaly) as well as multipeak structures in its temperature behavior, belongs among the most interesting features of frustrated magnetic systems intensively studied in the literature from the experimental as well as theoretical points of view (see, e.g., Refs. [1–30] and many others). The reason for this interest is at least twofold. On one hand, the very existence of these anomalies attracts attention because of the necessity of understanding their nature from a fundamental point of view and, on the other hand, the experimental interest is also given by the fact that anomalies of the specific heat capacity in frustrated magnetic systems are directly responsible for the very existence of strong magnetocaloric effects at low temperatures. Therefore, the corresponding materials are potentially very promising candidates for the effective adiabatic (de)magnetization cooling (see, e.g., Refs. [31–37] as well as references cited therein).

From the fundamental theoretical point of view, without doubt, the most valuable models of frustrated magnetic systems are those that can be exactly solved even in the presence of the external magnetic field because they can shed light on the fundamental physical nature of various specific properties of magnetic systems related to frustration, such as the formation of nontrivial systems of highly macroscopically degenerated ground states or strong magnetocaloric effects, which reveal themselves only in nonzero external magnetic fields.

In this respect, quite recently, the direct relation between the maximal number of peaks in the low-temperature behavior of the specific heat capacity and the dimensionality of the parametric space of a frustrated model was revealed in the framework of an exactly solvable antiferromagnetic Ising model in the external magnetic field on the kagome-like Husimi lattice [30]. Moreover, it was also shown there that the maximal possible number of peaks in the temperature dependence of the specific heat capacity in the corresponding regions of the model parametric space is directly related to the existence of strict hierarchies among the residual entropies of the neighboring ground states of all orders. Besides, in Ref. [38], the direct relation between the existence of highly macroscopically degenerated single-point ground states in frustrated models and the formation of the field-induced sharp double-peak structure in the low-temperature behavior of the specific heat capacity as a function of the external magnetic field was identified and studied in detail in the framework of the exactly solvable antiferromagnetic Ising model in the external magnetic field on the tetrahedron recursive lattice.

However, since all these results were obtained, on one hand, in the framework of models on recursive lattices and, on the other hand, in the framework of the models for which

the strict residual-entropy hierarchies are always valid, the following natural questions immediately arise here. The first of them is related to the relevance of the obtained results in Refs. [30,38] for the properties of frustrated systems on real lattices, i.e., whether the general results and conclusions obtained in Refs. [30,38] can also be considered as relevant for frustrated magnetic systems on standard regular lattices. The second nontrivial question is related to the behavior of the specific heat capacity in the situations in which there do not exist strict hierarchies between residual entropies of the neighboring ground states of different orders. It is clear that to be able to answer both these questions it is necessary, on one hand, to find an exactly solvable frustrated magnetic system on a regular lattice in the framework of which the anomalous properties of the specific heat capacity could be investigated and, on the other hand, to find a model with at least one violated strict hierarchy between residual entropies of neighboring ground states of different orders.

It is quite intriguing that there exists a model, namely, the antiferromagnetic Ising model with the multisite interaction in the external magnetic field on the so-called zigzag ladder [39], in the framework of which both these questions can be studied even simultaneously. This model has the same parametric space as the model studied in Ref. [30] and, moreover, as was shown in Ref. [39], it contains a single-point ground state whose residual entropy is the same as the residual entropies of two neighboring plateau-like ground states. In this respect, in the present paper, using the aforementioned model on the zigzag ladder, we shall show that all general conclusions about the low-temperature properties of the specific heat capacity obtained in the framework of the models on recursive lattices seem to be also valid on regular geometrically frustrated lattices. Besides, we shall also show that the absence of the strict hierarchy among residual entropies of the neighboring ground states of different orders, on one hand, leads to the reduction of the maximal possible number of peaks in the low-temperature behavior of the specific heat capacity in the corresponding regions of the parametric space of the model and, on the other hand, also leads to qualitatively substantially different behavior of the specific heat capacity as a function of the external magnetic field at low temperatures.

In the end, although the aim of the present paper is to describe and understand general properties of the specific heat capacity of frustrated magnetic systems but not to describe a concrete magnetic material, nevertheless let us note that results obtained in the framework of various classical and quantum models on the ladder-like lattices (see, e.g., Refs. [40–58] and references cited therein) are also important phenomenologically and can be used for theoretical description of properties of real physical systems such as $SrCuO_2$ [59,60], $SrCu_2O_3$ [61], $La_6Ca_8Cu_{24}O_{41}$ [62,63], $Cu_2(C_5H_{12}N_2)_2Cl_4$ [64], $KCuCl_3$ and $TlCuCl_3$ [65], NH_4CuCl_3 [66], Li_2CuO_2 and $CuGeO_3$ [63], $NaCu_2O_2$ [67], $La_8Cu_7O_{19}$ [68], $Cu(CF_3COO)_2$ [69], $Sr_2Co_3S_2O_3$ [70], and many others.

The paper is organized as follows. In Sec. II, the system of all ground states of the model is summarized and their convenient classification is introduced. In Sec. III, the exact expressions for the residual entropies of all model ground states are found. In Sec. IV, the properties of the specific heat capacity of the model are investigated in detail. Finally, the main results of the paper are summarized and discussed in Sec. V.

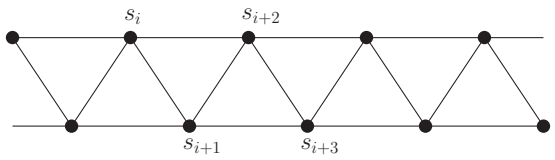

FIG. 1. The structure of the zigzag ladder.

II. THE MODEL AND ITS GROUND STATES

As was already mentioned in the Introduction, the main aim of this paper is to perform a detailed analysis of the influence of the violation of the strict residual-entropy hierarchy among neighboring ground states of different orders on the behavior of the specific heat capacity in frustrated magnetic systems. We shall investigate this problem in the framework of the exactly solvable geometrically frustrated antiferromagnetic spin-1/2 Ising model with the presence of the multisite interaction in the external magnetic field on the so-called zigzag ladder shown explicitly in Fig. 1.

The Hamiltonian of the model has the following form,

$$\mathcal{H} = -J \sum_{\langle i\,j\rangle} s_i s_j - J' \sum_{\langle i\,j\,k\rangle} s_i s_j s_k - H \sum_i s_i, \qquad (1)$$

where each variable s_i acquires one of two possible values ± 1, J represents the antiferromagnetic ($J < 0$) nearest-neighbor interaction parameter, J' is the multisite interaction within each single triangle, and H is the external magnetic field. Besides, the first sum in Eq. (1) runs over all nearest-neighbor spin pairs, the second sum runs over all triangles, and the third sum runs over all spin sites.

The model is exactly solvable [39] and, using the transfer matrix method, the partition function of the model can be written as follows,

$$Z_N = \mathrm{Tr} V^{N/2}, \qquad (2)$$

where N is the even number of all sites of the lattice with the standard periodic boundary condition $s_{N+i} = s_i$ and the transfer matrix V has the form

$$V = \begin{pmatrix} a^4bc^2 & ac & (ab)^{-1}c & a^{-2} \\ (ab)^{-1}c & 1 & a^{-2}b & ac^{-1} \\ ac & a^{-2}b^{-1} & 1 & b(ac)^{-1} \\ a^{-2} & b(ac)^{-1} & ac^{-1} & a^4b^{-1}c^{-2} \end{pmatrix}, \qquad (3)$$

and

$$a = e^K, \quad b = e^{2K'}, \quad c = e^h, \qquad (4)$$

where $K = \beta J$, $K' = \beta J'$, $h = \beta H$, $\beta = 1/(k_B T)$, T is the temperature, and k_B is the Boltzmann constant.

In the thermodynamical limit $N \to \infty$, the properties of the model are driven by the largest eigenvalue λ_1 of the transfer matrix (3), the explicit form of which is given as

follows:

$$\lambda_1 = \frac{1}{4}\left[k_1 + 2\sqrt{z_1 + w_1} + \sqrt{4(2z_1 - w_1) + \frac{z_2}{\sqrt{z_1 + w_1}}}\right], \tag{5}$$

where

$$k_1 = 2 + a^4\left(bc^2 + \frac{1}{bc^2}\right),$$

$$w_1 = \frac{1}{3}\left[\left(\frac{w_2}{2}\right)^{1/3} + z_3\left(\frac{2}{w_2}\right)^{1/3}\right],$$

$$z_1 = \frac{k_1^2}{4} - \frac{2k_4}{3},$$

$$z_2 = k_1^3 - 4k_1k_4 - 8k_3,$$

and

$$w_2 = z_4 + \sqrt{z_4^2 - 4z_3^3},$$

$$z_3 = k_4^2 + 12k_2 + 3k_1k_3,$$

$$z_4 = 2k_4^3 + 9\left[3\left(k_1^2k_2 + k_3^2\right) + k_4(k_1k_3 - 8k_2)\right],$$

$$k_2 = [b^2(1 + a^8) - a^4(1 + b^4)]^2/(a^8b^4),$$

$$k_3 = -\{b^2(b^2 - a^4)^2 + 2a^4bc^2[b^2(1 + a^8) - a^4(1 + b^4)] + c^4(a^4b^2 - 1)^2\}/(a^4b^3c^2),$$

$$k_4 = \{2a^4[a^4 - b^2 + c^4(a^4b^2 - 1)] + bc^2(a^{12} + a^4 - 2)\}/(a^4bc^2),$$

with a, b, and c defined in Eq. (4). Note that the existence of the unique largest real eigenvalue of the transfer matrix (3) follows from the well-known Perron-Frobenius theorem.

Thus, in the limit $N \to \infty$, the partition function of the model obtains the following form,

$$Z = \lambda_1^{N/2}, \quad N \to \infty, \tag{6}$$

and, finally, the free energy per site is given as follows:

$$f \equiv -\lim_{N\to\infty} \frac{\ln Z_N}{\beta N} = -\frac{\ln \lambda_1}{2\beta}. \tag{7}$$

The exact solution of the model was discussed recently, e.g., in Ref. [39], where a complete analysis of the magnetization properties of the model was performed, the system of all ground states was identified, and the existence of the so-called single-point ground states with well-defined thermodynamic properties was shown. In Ref. [39], the exact expressions for the magnetization of all ground states were found and a brief discussion of numerical values of their residual entropies was performed. Because, in what follows, we shall intensively use the results obtained in Ref. [39], it is therefore appropriate to summarize them briefly and, at the same time, to introduce a convenient notation and classification of the system of the ground states of the model.

As was shown in Ref. [39], in the limit $T \to 0$, the model described by the Hamiltonian (1) on the zigzag ladder exhibits the existence of three qualitatively different plateau-like ground states with absolute values of magnetization $|m| = 0, 1/3$, and 1. In addition, the model also exhibits the existence of six qualitatively different single-point ground states,

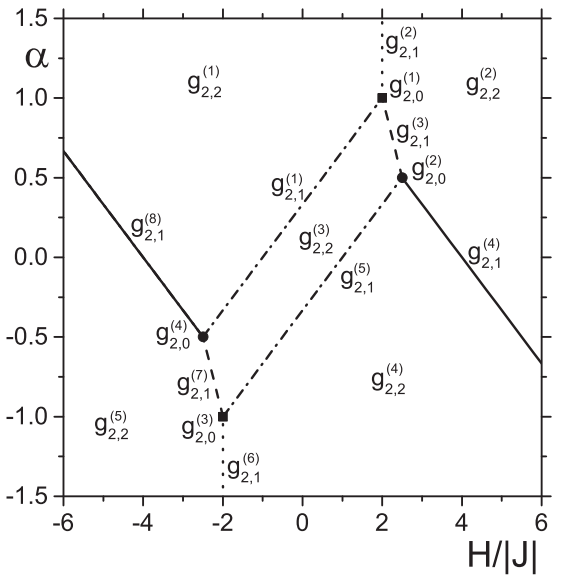

FIG. 2. The system of all ground states of the model in the plane $H/|J|$ versus $\alpha = J'/|J|$ (see the text for used notation). Their magnetization properties are summarized in Table I.

which are realized on the corresponding lines that form borders between various neighboring plateau-like ground states and at four separated points at which three different plateaus (or the corresponding border lines) meet (see Fig. 2). The magnetization properties of all ground states of the model are summarized in Table I.

Using a convenient general classification of the ground states of frustrated systems introduced in Ref. [30], the studied model, in fact, exhibits the existence of three different types of the ground states, which are realized in the corresponding regions of the ground-state parametric space with different spatial dimensions. In accordance with this general terminology and classification, the studied model has two-dimensional ground-state parametric space $\mathcal{G}_2$, which is characterized by two independent dimensionless parameters $H/|J|$ and $\alpha \equiv J'/|J|$, in which the set of all possible ground states G_2 of the model is realized. At the same time, the set of all ground states of the model G_2 can be naturally divided into three disjunct subsets $G_{2,i}$, $i = 0, 1, 2$ ($G_2 = \bigcup_{i=0}^{2} G_{2,i}$), such that, for given value of i, the subset $G_{2,i}$ contains the ground states of the ith order that are realized on the corresponding i-dimensional segments of the parametric space $\mathcal{G}_2$. Thus, as follows from Fig. 2, the subset $G_{2,0} = \{g_{2,0}^{(1)}, \ldots, g_{2,0}^{(4)}\}$ contains the zeroth-order ground states that are realized at the four separate points (the zero-dimensional objects) in the parametric space $\mathcal{G}_2$, the subset $G_{2,1} = \{g_{2,1}^{(1)}, \ldots, g_{2,1}^{(8)}\}$ contains the first-order ground states that are realized on the eight different line segments (the one-dimensional objects), and, finally, the subset $G_{2,2} = \{g_{2,2}^{(1)}, \ldots, g_{2,2}^{(5)}\}$ contains all ground states of the second order that are realized in the two-dimensional regions of the parametric space. Moreover, as is also evident from Fig. 2, the corresponding i-dimensional object $\mathfrak{g}_{2,i}^{(j)}$ in the whole parametric space can be uniquely associated with the ground state $g_{2,i}^{(j)}$; i.e., the ground state $g_{2,i}^{(j)}$, for given values i and j, is realized for all values of

TABLE I. Survey of the magnetization properties of all ground sates of the model together with their residual entropies.

$G_{2,0}$		$g^{(1)}_{2,0}$	$g^{(2)}_{2,0}$	$g^{(3)}_{2,0}$	$g^{(4)}_{2,0}$
	m	0.222984	0.447214	−0.222984	−0.447214
	s/k_B	0.382245	0.481212	0.382245	0.481212

$G_{2,1}$		$g^{(1)}_{2,1}$	$g^{(2)}_{2,1}$	$g^{(3)}_{2,1}$	$g^{(4)}_{2,1}$	$g^{(5)}_{2,1}$	$g^{(6)}_{2,1}$	$g^{(7)}_{2,1}$	$g^{(8)}_{2,1}$
	m	0.159320	1/3	0.396651	0.611492	−0.159320	−1/3	−0.396651	−0.611492
	s/k_B	0.199461	0	0.322285	0.382245	0.199461	0	0.322285	0.382245

$G_{2,2}$		$g^{(1)}_{2,2}$	$g^{(2)}_{2,2}$	$g^{(3)}_{2,0}$	$g^{(4)}_{2,2}$	$g^{(5)}_{2,2}$
	m	−1/3	1	0	1/3	−1
	s/k_B	0	0	0	0	0

the model parameters from the ground-state parametric space segment $\mathfrak{g}^{(j)}_{2,i}$. Thus, in our case, the whole parametric space $\mathcal{G}_2$ can also be uniquely written in the form $\mathcal{G}_2 = \bigcup_{i=0}^{2} \mathcal{G}_{2,i}$, where $\mathcal{G}_{2,i}$ represents the union of all regions $\mathfrak{g}^{(j)}_{2,i}$ in which the corresponding ith-order ground states $g^{(j)}_{2,i}$ are realized.

Here it is necessary to stress that the exact one-to-one correspondence between disjunct segments $\mathfrak{g}^{(j)}_{2,i} \subset \mathcal{G}_2$ and elements $g^{(j)}_{2,i} \in G_2$ is a direct consequence of the nonexistence of first-order phase transitions in the studied model, i.e., of the fact that the model exhibits the single solution for arbitrary model parameter values. In general, of course, such kind of one-to-one correspondence is not always obvious.

Note also that, in what follows, the concept of *the neighboring ground states of different orders* will play the central role; therefore it is instructive to define its exact meaning. Thus, in the sense of the above given classification of the system of the ground states of the model, two ground states $g^{(k)}_{2,i}$ and $g^{(l)}_{2,j}$ of different orders $i < j$ are *the neighboring ground states* if the corresponding region $\mathfrak{g}^{(k)}_{2,i}$ of the parametric space of the model, in which the ground state $g^{(k)}_{2,i}$ is realized, is a part of the border of the region $\mathfrak{g}^{(l)}_{2,j}$, in which the higher-order ground state $g^{(l)}_{2,j}$ is formed.

As we shall see, namely the hierarchical ordering of neighboring ground states of the model discussed above, together with the existence of nontrivial residual-entropy hierarchies among neighboring ground states of different orders, is crucial for the fundamental understanding of its thermodynamic behavior, especially for low-temperature properties of various phenomenologically interesting anomalies of the specific heat capacity. In this respect, the terminology and classification given above will be used intensively in what follows.

However, before we investigate in detail the properties of the specific heat capacity of the model it is necessary first to analyze systematically the entropy properties of the model together with the exact determination of the residual entropies of all ground states. This analysis is performed in detail in the next sections.

III. EXACT EXPRESSIONS FOR RESIDUAL ENTROPIES OF ALL GROUND STATES

As was mentioned above, the properties of the entropy per site of the model play the central role in the fundamental understanding of the behavior of the specific heat capacity, especially as for its anomalous behavior at low temperatures. Therefore, it is desirable to analyze them in detail.

However, for our purposes, it is more convenient to investigate the behavior of the entropy of the model as a function of the temperature as well as of the external magnetic field simultaneously with the corresponding investigation of the properties of the specific heat capacity, which will be given in the next section. Therefore, in the present section, we shall restrict our attention to the determination of the exact values for the residual entropies of all ground states of the model, which will be important in what follows.

Thus, using the explicit expression for the free energy per site given in Eq. (7) (see also Ref. [39]), the entropy per site of the model can be written as follows:

$$s \equiv -\frac{\partial f}{\partial T} = \frac{k_B}{2}\left(\ln \lambda_1 + \frac{T}{\lambda_1}\frac{\partial \lambda_1}{\partial T}\right), \tag{8}$$

where λ_1 is given in Eq. (5).

First of all, as expected, the residual entropy of all plateau-like ground states with values of magnetization $m = 0, \pm 1/3$, and ± 1, i.e., of all ground states of the second order $G_{2,2}$, is zero.

On the other hand, the exact expressions for residual entropies of the first-order ground states $G_{2,1}$ are the following: The explicit form of the residual entropy of the ground states $g^{(1)}_{2,1}$ and $g^{(5)}_{2,1}$, i.e., of the ground states that are realized on the corresponding lines $\mathfrak{g}^{(1)}_{2,1}$ and $\mathfrak{g}^{(5)}_{2,1}$ in the limit $T \to 0$ with absolute value of magnetization $|m| \approx 0.159320$ (the dash-dotted lines in Fig. 2), is

$$s = \frac{k_B}{2} \ln\left[\frac{1}{2\sqrt{6}}(\sqrt{y_1} + \sqrt{y_2 + 12\sqrt{6/y_1}})\right], \tag{9}$$

where

$$y_1 = 8 + 32(2/z_1)^{1/3} + (4z_1)^{1/3}, \tag{10}$$

$$y_2 = 16 - 32(2/z_1)^{1/3} - (4z_1)^{1/3}, \tag{11}$$

and

$$z_1 = 155 + 3\sqrt{849}. \tag{12}$$

Its approximate numerical value is $s \approx 0.199461 k_B$.

The residual entropy of the ground states $g^{(3)}_{2,1}$ and $g^{(7)}_{2,1}$, i.e., of the ground states that are realized on lines $\mathfrak{g}^{(3)}_{2,1}$ and $\mathfrak{g}^{(7)}_{2,1}$

with the absolute value of magnetization $|m| \approx 0.396651$ (the dashed lines in Fig. 2), has the following form:

$$s = \frac{k_B}{2} \ln \left\{ \frac{1}{2} \left[\frac{1}{2} + \sqrt{y_3} + \sqrt{y_4 + 9/(4\sqrt{y_3})} \right] \right\}, \quad (13)$$

where

$$y_3 = [19/4 + 16(2/z_1)^{1/3} + (z_1/2)^{1/3}]/3, \quad (14)$$

$$y_4 = [19/2 - 16(2/z_1)^{1/3} - (z_1/2)^{1/3}]/3, \quad (15)$$

and z_1 is again given in Eq. (12). Its approximate value is $s \approx 0.322285 k_B$.

Further, the residual entropy of the ground states $g_{2,1}^{(4)}$ and $g_{2,1}^{(8)}$, i.e., of the ground states that are realized on lines $\mathfrak{g}_{2,1}^{(4)}$ and $\mathfrak{g}_{2,1}^{(8)}$ with the absolute value of magnetization $|m| \approx 0.611492$ (the solid lines in Fig. 2), is given as follows:

$$s = \frac{k_B}{2} \ln \left\{ \frac{1}{12} \left[3 + \sqrt{3y_5} + \sqrt{6(y_6 + 51\sqrt{3/y_5})} \right] \right\}, \quad (16)$$

where

$$y_5 = 19 + 4(2/z_2)^{1/3} + 2(4z_2)^{1/3}, \quad (17)$$

$$y_6 = 19 - 2(2/z_2)^{1/3} - (4z_2)^{1/3}, \quad (18)$$

and

$$z_2 = 29 + 3\sqrt{93}. \quad (19)$$

Its approximate value is $s \approx 0.382245 k_B$.

The last kind of the first-order ground states are $g_{2,1}^{(2)}$ and $g_{2,1}^{(6)}$. They are realized on the corresponding lines $\mathfrak{g}_{2,1}^{(2)}$ and $\mathfrak{g}_{2,1}^{(6)}$ with the absolute value of magnetization $|m| = 1/3$ (the dotted lines in Fig. 2) and they have the same residual entropy as the corresponding neighboring plateau-like ground states; i.e., their entropy is equal to zero. This means that, in this case, one is faced with a nontrivial and rather specific situation in which the neighboring ground states of different orders do not exhibit residual-entropy difference; i.e., the residual-entropy hierarchy among neighboring different-order ground states is violated. As we shall see, this fact has nontrivial consequences for behavior of the specific heat capacity in the vicinity of these first-order ground states.

Finally, let us find the residual entropies of the zeroth-order ground states belonging to $G_{2,0}$. It is quite interesting that the zeroth-order ground states $g_{2,0}^{(1)}$ and $g_{2,0}^{(3)}$, which are realized at two points $\mathfrak{g}_{2,0}^{(1)}$ and $\mathfrak{g}_{2,0}^{(3)}$ in the parametric space (the filled squares in Fig. 2), have the same value of the residual entropy $s \approx 0.382245 k_B$ as the first-order ground states $g_{2,1}^{(4)}$ and $g_{2,1}^{(8)}$ [i.e., the exact expression for this residual entropy is also given by Eq. (16)], although their absolute value of the magnetization $|m| \approx 0.222984$ is completely different. This means that the macroscopic degeneracy of these ground states of different orders is also the same. However, in this case, as we shall see, this fact has no impact on the behavior of the specific heat capacity in their vicinity because they are not neighboring ground states of different orders.

The last type of the zeroth-order ground states is represented by the ground states $g_{2,0}^{(2)}$ and $g_{2,0}^{(4)}$, which are again realized at two discrete points $\mathfrak{g}_{2,0}^{(2)}$ and $\mathfrak{g}_{2,0}^{(4)}$ in the parametric space denoted as the filled circles in Fig. 2, with the absolute value of magnetization $|m| \approx 0.447214$. Their residual entropy is given as follows:

$$s = \frac{k_B}{2} \ln \left[\frac{3 + \sqrt{5}}{2} \right], \quad (20)$$

with the approximate numerical value $s \approx 0.481212 k_B$.

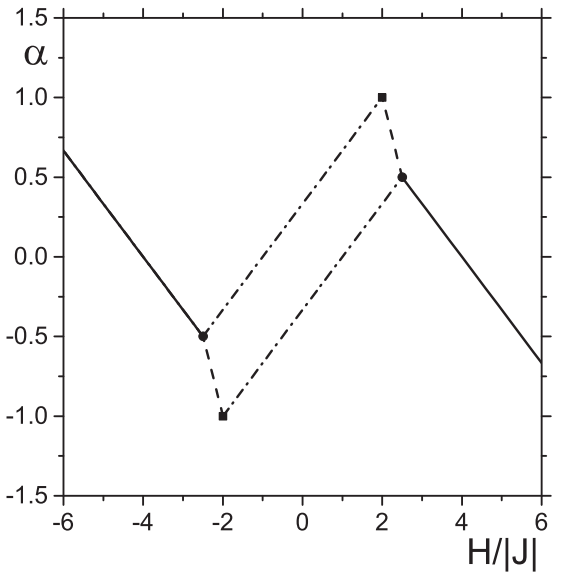

FIG. 3. The system of the ground states with different residual entropies. The values of all residual entropies are summarized in Table I (see Fig. 2 for notation).

For clarity and completeness, the residual entropies of all ground states of the model together with their magnetization properties are summarized in Table I.

One of the most important conclusions that follows from the investigation of the residual entropies of the model is the fact that the entropy picture of the ground states in the model parametric space is different than the corresponding picture from the magnetization point of view. While the system of the ground states from the magnetization point of view is given in Fig. 2, the system of all different residual entropies of the neighboring ground states is shown explicitly in Fig. 3. The absence of lines $\mathfrak{g}_{2,1}^{(2)}$ and $\mathfrak{g}_{2,1}^{(6)}$ in Fig. 3 (the dotted lines in Fig. 2) demonstrates the violation of the strict residual-entropy hierarchy among the corresponding neighboring ground states of different orders (see also Table I). More precisely, one says that the residual-entropy hierarchy between the neighboring ground states $g_{2,i}^{(k)}$ and $g_{2,i+1}^{(l)}$ is strict if the residual entropy of the ith-order ground state is greater than the residual entropy of the ground state of the order $i+1$. On the other hand, the strict residual-entropy hierarchy between these neighboring ground states is violated if their residual entropies are equal.

The system of all residual-entropy hierarchies among neighboring ground states of different orders is schematically shown in Fig. 4. In this figure, various ground states are denoted by the corresponding filled blue (the zeroth-order ground states $g_{2,0}^{(i)}$), red (the first-order ground states $g_{2,1}^{(i)}$), and green (the second-order ground states $g_{2,2}^{(i)}$) circles. Besides,

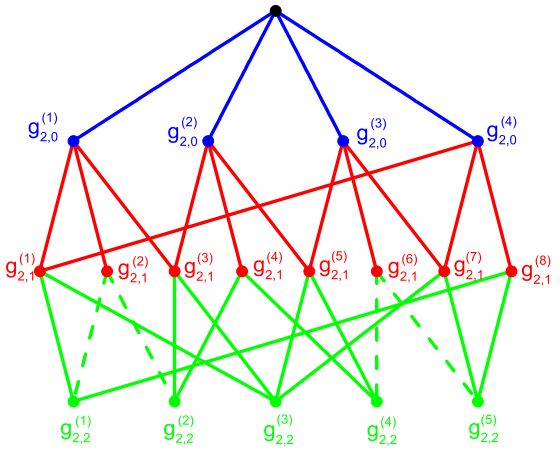

FIG. 4. The symbolic demonstration of all residual-entropy hierarchies among the neighboring ground states of different orders. The neighboring ground states of different orders [represented by the blue ($g^{(i)}_{2,0}$), red ($g^{(i)}_{2,1}$), and green ($g^{(i)}_{2,2}$) filled circles] with strict residual-entropy hierarchy are connected by the solid lines (the red lines between $g^{(i)}_{2,0}$ and $g^{(j)}_{2,1}$ and the green lines between $g^{(i)}_{2,1}$ and $g^{(j)}_{2,2}$). The neighboring ground states of different orders with violated residual-entropy hierarchy are connected by the dashed (green) lines. The upper black filled circle represents the entropy per site $k_B \ln 2$ of the fully disordered state obtained for $T \to \infty$, and the blue solid lines (the lines between the upper black filled circle and all blue filled circles that correspond to $g^{(i)}_{2,0}$) represent strict entropy hierarchies between this maximal entropy and the residual entropies of all zeroth-order ground states $g^{(i)}_{2,0}$. Namely, the existence of these last hierarchies is responsible for the very existence of the standard peak in the temperature dependence of the specific heat capacity.

the upper black filled circle represents the fully disordered state of the system with entropy $k_B \ln 2$. Each connection between various ground states of different orders, i.e., each green (the lines between $g^{(i)}_{2,1}$ and $g^{(j)}_{2,2}$) and red (the lines between $g^{(i)}_{2,0}$ and $g^{(j)}_{2,1}$) line, means that the corresponding ground states are neighboring ground states in the ground-state parametric space. At the same time, the neighboring ground states of different orders with strict residual-entropy hierarchies (i.e., for which the ground state of lower order has larger residual entropy than the corresponding neighboring ground state of higher order) are connected by the solid lines and, on the other hand, the neighboring ground states of different orders with violated residual-entropy hierarchy (i.e., their residual entropy is the same) are connected by the dashed lines. In addition, the solid blue lines (the lines between $g^{(i)}_{2,0}$ and the upper black filled circle) represent the strict entropy hierarchies between all zeroth-order ground states $g^{(i)}_{2,0}$ and the maximal possible entropy of any two-state statistical system. As we shall see, namely, the existence of these last hierarchies is responsible for the very existence of the standard peak in the behavior of the specific heat capacity as a function of the temperature.

Thus, the present model exhibits two qualitatively different situations that are directly related to the strength of the multisite interaction. When the multisite interaction is weaker or equal to the nearest-neighbor antiferromagnetic interaction, i.e., when $|\alpha| \leqslant 1$, then all neighboring ground states of different orders exhibit strict hierarchies of their residual entropies; i.e., the residual entropy of a lower-order ground state is always greater than the residual entropies of all neighboring ground states of higher orders. On the other hand, when $|\alpha| > 1$, there exist the neighboring ground states of different orders for which the residual-entropy hierarchy is absent. In what follows, our aim is to investigate the influence of this residual entropy hierarchy violation on the properties of the behavior of the specific heat capacity for the parameters of the model from the vicinity of these single-point ground states and to compare it to the standard situation when the corresponding hierarchies are strict, as was discussed in detail in Ref. [30].

IV. RELATION BETWEEN FORMATION OF RESIDUAL ENTROPY HIERARCHIES AND PROPERTIES OF LOW-TEMPERATURE ANOMALIES OF SPECIFIC HEAT CAPACITY

In Ref. [30], the direct relation between the very existence of residual-entropy hierarchies among neighboring ground states of various orders and low-temperature anomalies of the specific heat capacity was identified and demonstrated in the framework of a model in which all residual-entropy hierarchies are strict. There, it was shown that if one studies a model, in general, with n-dimensional ground-state parametric space, then the specific heat capacity as a function of the temperature can exhibit at most $i+1$ peaks when the parameters of the model are taken from regions that form $\mathcal{G}_{n,i}$. Thus, the maximal possible number of peaks in the temperature behavior of the specific heat capacity, which can be observed in a frustrated model with n-dimensional ground-state parametric space, is equal to $n+1$ and can be observed only for model parameters from regions that form $\mathcal{G}_{n,n}$ but only in the case when, at least, one strict residual-entropy hierarchy exists among neighboring ground states of all orders. Moreover, when, in a model with n-dimensional ground-state parametric space, all residual-entropy hierarchies among neighboring ground states of all orders are strict, then each region from $\mathcal{G}_{n,i}$ is divided into subregions in which the specific heat capacity exhibits all number of peaks up to $i+1$. At the same time, in this case, the subregion of a region from $\mathcal{G}_{n,i}$, where the specific heat capacity exhibits j-peak structure, is always bordering with subregions of the corresponding regions from $\mathcal{G}_{n,i+1}$, where the temperature behavior of the specific heat capacity exhibits $j+1$ peaks. All these facts were demonstrated in Ref. [30] in the framework of an exactly solvable frustrated model with two-dimensional ground-state parametric space, where all subregions of the model parametric space, for which the specific heat capacity exhibits one-, two-, and three-peak structure, were identified (see Figs. 15 and 16 in Ref. [30]).

The open question, however, is what will change in this picture when, at least, one residual-entropy hierarchy among neighboring ground states of all orders is not strict, i.e., when, at least, one residual entropy of a ground state of the ith order is equal to the residual entropy of the neighboring ground state of the order $i+1$. Namely, such a situation is observed in the model given by Hamiltonian (1) on the zigzag ladder studied in this paper. Here, as was shown in the previous section, the residual entropy of the ground states $g^{(2)}_{2,1}$ and $g^{(6)}_{2,1}$, which are

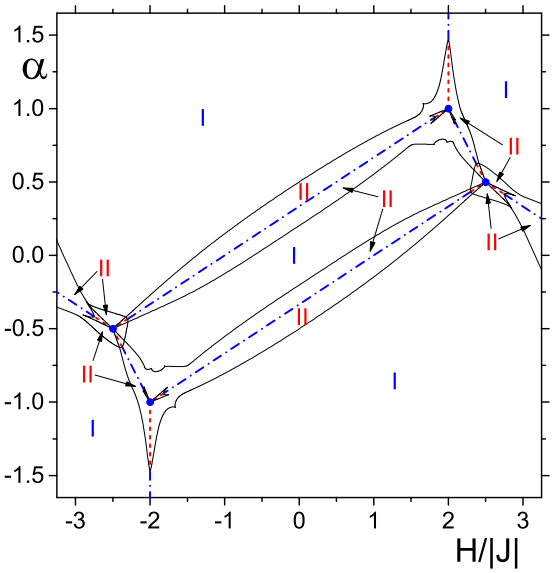

FIG. 5. The regions of the parameters of the model for which the specific heat capacity exhibits one-peak (the blue filled circle, the blue dash-dotted lines, and the two-dimensional regions denoted by blue Roman numeral I), two-peak (the dashed red lines and the two-dimensional regions denoted by red Roman numeral II), and three-peak (not denoted explicitly in this figure) behavior as a function of the temperature. The regions where three peaks are formed in the temperature behavior of the specific heat capacity can be also seen here although are not denoted. They are shown and denoted explicitly in detailed Figs. 7 and 8 of the regions in the vicinity of the zeroth-order ground states $g^{(2)}_{2,0}$ and $g^{(1)}_{2,0}$, respectively, where they are denoted by green Roman numeral III.

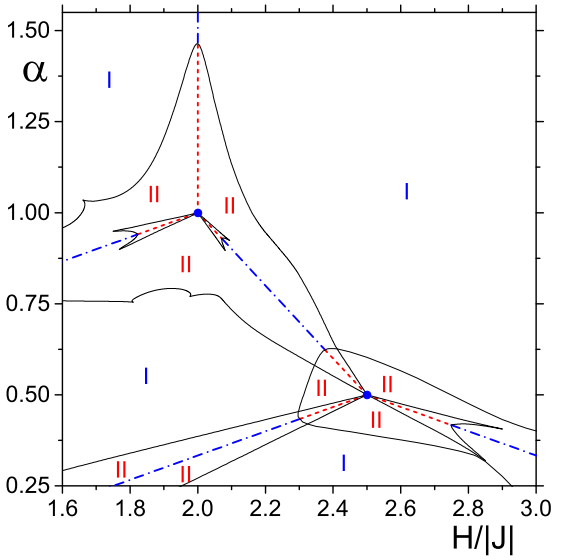

FIG. 6. Detailed illustration of the regions of the model parameters in the vicinity of the zeroth-order ground states $g^{(1)}_{2,0}$ and $g^{(2)}_{2,0}$ (blue filled circles) for which the specific heat capacity exhibits one-peak (the blue filled circle, the blue dash-dotted lines, and the two-dimensional regions denoted by blue Roman numeral I), two-peak (the dashed red lines and the two-dimensional regions denoted by red Roman numeral II), and three-peak (not denoted explicitly in this figure) behavior as a function of the temperature. The regions where three peaks are formed in the temperature behavior of the specific heat capacity can be also seen here although they are not denoted. They are shown and denoted explicitly in detailed Figs. 7 and 8, respectively, where they are denoted by green Roman numeral III.

realized on the line segments $\mathfrak{g}^{(2)}_{2,1}$ and $\mathfrak{g}^{(6)}_{2,1}$ (see Fig. 2), is equal to the residual entropy of the corresponding neighboring ground states $g^{(1)}_{2,2}$ and $g^{(2)}_{2,2}$ and $g^{(4)}_{2,2}$ and $g^{(5)}_{2,2}$, respectively (see Figs. 2–4 as well as Table I). This fact has nontrivial impact on the behavior of the specific heat capacity for the model parameters from the vicinity of these line segments.

In this respect, in Figs. 5–8, the regions of the ground-state parametric space of the model, in which various ground states are realized, are divided into subregions in which one-, two-, and three-peak structure in the behavior of the specific heat capacity as a function of the temperature is observed. As was already discussed, for values of model parameters for which the ith-order ground states are formed in the limit $T \to 0$, one can observe at most $i+1$-peak structure in the temperature behavior of the specific heat capacity. As follows from Figs. 5–8, the one-peak structure in the behavior of the specific heat capacity is observed at all points where the zeroth-order ground states are formed, i.e., for all model parameters that correspond to the set $\mathcal{G}_{2,0}$ (filled blue circles in Figs. 5–8). On the other hand, on the geometric objects in the ground-state parametric space of the model, where the ground states of the first order are formed in the zero-temperature limit, i.e., on all line segments belonging to $\mathcal{G}_{2,1}$, at most two-peak structure in the temperature behavior of the specific heat capacity can be observed. Due to the fact that the residual-entropy hierarchies between all ground states of the first order and the corresponding neighboring ground states of the zeroth order are strict, each line segment $\mathfrak{g}^{(i)}_{2,1}$, $i = 1, \ldots, 8$, is uniquely divided into subregions with the one-peak [the dash-dotted (blue) lines in Figs. 5–8] and the two-peak [the dashed (red) lines in Figs. 5–8] structure in the behavior of the specific heat capacity. At the same time, the subregions with the two-peak structure in the behavior of the specific heat capacity are adjoining to the corresponding point from $\mathcal{G}_{2,0}$. To be more concrete, the coordinates of the points that separate subregions of the corresponding line segments from the set $\mathcal{G}_{2,1}$, where the one- and two-peak structures in the behavior of the specific heat capacity are realized, are the following: the coordinates of these points are $\{H/|J|, \alpha\} \approx \{\pm 2, \pm 1.467\}$ for lines $\mathfrak{g}^{(2)}_{2,1}$ and $\mathfrak{g}^{(6)}_{2,1}$; $\{H/|J|, \alpha\} \approx \{\pm 2.749, \pm 0.417\}$ for lines $\mathfrak{g}^{(4)}_{2,1}$ and $\mathfrak{g}^{(8)}_{2,1}$; $\{H/|J|, \alpha\} \approx \{\pm 2.071, \pm 0.929\}$ and $\{H/|J|, \alpha\} \approx \{\pm 2.377, \pm 0.623\}$ for lines $\mathfrak{g}^{(3)}_{2,1}$ and $\mathfrak{g}^{(7)}_{2,1}$; and the coordinates of two separating points are $\{H/|J|, \alpha\} \approx \{\pm 1.823, \pm 0.941\}$ and $\{H/|J|, \alpha\} \approx \{\mp 2.302, \mp 0.434\}$ for lines $\mathfrak{g}^{(1)}_{2,1}$ and $\mathfrak{g}^{(5)}_{2,1}$.

Finally, the maximal possible number of peaks in the temperature behavior of the specific heat capacity for the parameters of the model from regions that form $\mathcal{G}_{2,2}$, i.e., where the second-order ground states are formed in the zero-temperature limit, is three. At the same time, the three-peak structure of the specific heat capacity is maximally possible in the framework of the studied model with the two-dimensional ground-state parametric space. As was discussed in detail in Ref. [30], the three-peak structure in the behavior of the specific heat capacity emerges only in restricted areas adjoining the line segments of $\mathfrak{g}^{(i)}_{2,1}$, $i =$

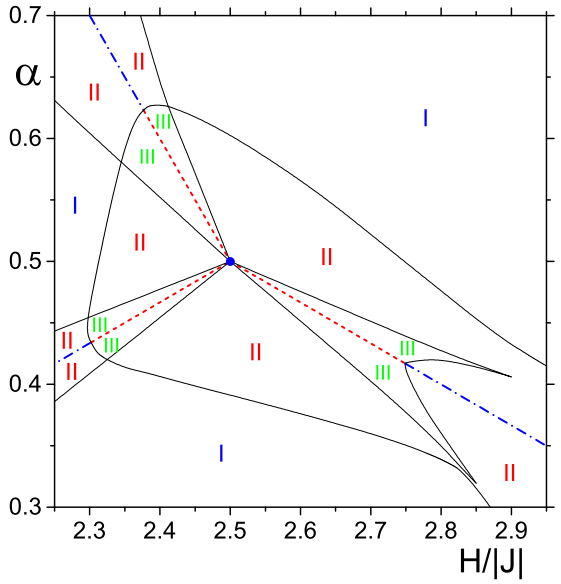

FIG. 7. Detailed illustration of the regions of the model parameters in the vicinity of the zeroth-order ground state $g^{(2)}_{2,0}$ (blue filled circle) for which the specific heat capacity exhibits one-peak (the blue filled circle, the blue dash-dotted lines, and the two-dimensional regions denoted by blue Roman numeral I), two-peak (the dashed red lines and the two-dimensional regions denoted by red Roman numeral II), and three-peak (the two-dimensional regions denoted by the green Roman numeral III) behavior as a function of the temperature.

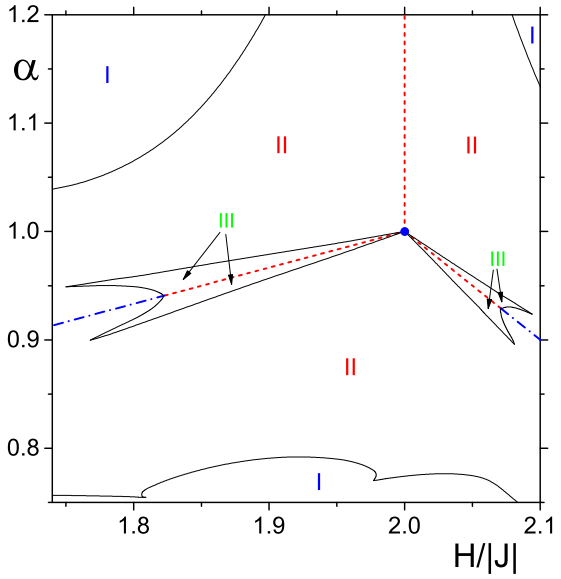

FIG. 8. Detailed illustration of the regions of the model parameters in the vicinity of the zeroth-order ground state $g^{(1)}_{2,0}$ (blue filled circle) for which the specific heat capacity exhibits one-peak (the blue filled circle, the blue dash-dotted lines, and the two-dimensional regions denoted by blue Roman numeral I), two-peak (the dashed red lines and the two-dimensional regions denoted by red Roman numeral II), and three-peak (the two-dimensional regions denoted by the green Roman numeral III) behavior as a function of the temperature.

$1, \ldots, 8$, where the specific heat capacity exhibits two-peak structure in its temperature behavior, but only in the case in which there is a strict residual-entropy hierarchy among the corresponding neighboring ground states of all orders. In our model, as was already mentioned, the strict residual-entropy hierarchies are valid in all cases when $|\alpha| \leqslant 1$. As a consequence, the regions with the three-peak structure in the temperature behavior of the specific heat capacity exist in the vicinity of each line segment of $\mathfrak{g}^{(i)}_{2,1}$, $i = 1, 3, 4, 5, 7, 8$, where the two-peak structure in the behavior of the specific heat capacity is observed (see the corresponding regions in Figs. 5–8 denoted by green Roman numeral III in Figs. 7 and 8). At the same time, the two-peak structure in the temperature behavior of the specific heat capacity is observed in the subregions of all regions that form $\mathcal{G}_{2,2}$ adjoining the corresponding line segments of $\mathfrak{g}^{(i)}_{2,1}$, $i = 1, 3, 4, 5, 7, 8$, where the one-peak structure in the behavior of the specific heat capacity is observed as well as adjoining to the regions where the three-peak structure in the specific heat capacity is observed (see the corresponding regions in Figs. 5–8 denoted by red Roman numeral II). In remaining subregions of the regions that form $\mathcal{G}_{2,2}$ (denoted by blue Roman numeral I in Figs. 5–8), the specific heat capacity exhibits standard one-peak behavior.

However, when $|\alpha| > 1$, the strict residual-entropy hierarchies between the first-order ground states $g^{(2)}_{2,1}$ and $g^{(6)}_{2,1}$ and the corresponding neighboring second-order ground states $g^{(1)}_{2,2}$ and $g^{(2)}_{2,2}$ and $g^{(4)}_{2,2}$ and $g^{(5)}_{2,2}$, respectively, are violated (see Figs. 3 and 4 and the corresponding discussion in the previous section) because all these ground states have the same value of the entropy per site equal to zero. This fact has substantial consequences on the behavior of the specific heat capacity for the model parameters from the vicinity of line segments $\mathfrak{g}^{(2)}_{2,1}$ and $\mathfrak{g}^{(6)}_{2,1}$, where the first-order ground states $g^{(2)}_{2,1}$ and $g^{(6)}_{2,1}$ are formed. This can be seen immediately in Figs. 5, 6, and 8. In this case, there exist no subregions of regions $\mathfrak{g}^{(1)}_{2,2}$, $\mathfrak{g}^{(2)}_{2,2}$, $\mathfrak{g}^{(4)}_{2,2}$, and $\mathfrak{g}^{(5)}_{2,2}$ that, on one hand, would be adjoining $\mathfrak{g}^{(2)}_{2,1}$ and $\mathfrak{g}^{(6)}_{2,1}$, respectively, and, on the other hand, at the same, the specific heat capacity would exhibit the three-peak structure as a function of the temperature. Thus, in this case, the maximal number of peaks in the temperature behavior of the specific heat capacity is reduced by one, i.e., by the number of residual-entropy hierarchy violations.

As will be shown in what follows, the nonexistence of the strict residual-entropy hierarchy between some neighboring ground states of different orders has nontrivial impact not only on the number of peaks in the temperature behavior of the specific heat capacity but also on the qualitative as well as quantitative behavior of the specific heat capacity as a function of the external magnetic field.

First of all, let us analyze typical behavior of the specific heat capacity as a function of the temperature in the vicinity of the zeroth-order ground states of the model in situations when strict residual-entropy hierarchies among neighboring ground states of different orders are valid. In this respect, in Figs. 9–11, the typical temperature behavior of the specific heat capacity for parameters from the vicinity of points $\mathfrak{g}^{(1)}_{2,0}$ and $\mathfrak{g}^{(2)}_{2,0}$ of the parametric space, where the zeroth-order ground states $g^{(1)}_{2,0}$ and $g^{(2)}_{2,0}$ are formed, is demonstrated. The

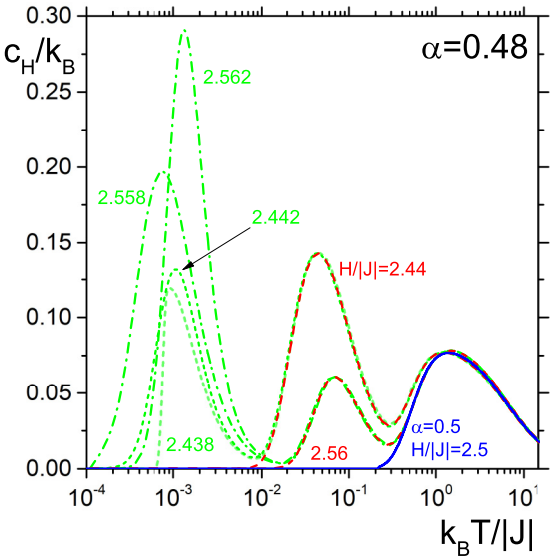

FIG. 9. The behavior of the specific heat capacity as a function of the reduced temperature for parameter $\alpha = 0.48$ and for six representative values of the external magnetic field chosen from six different regions of the parametric space where two and three peaks are formed, namely, for $H/|J| = 2.44$ and 2.56 (the red dashed curves) for which two-peak structure is formed and for $H/|J| = 2.438$ and 2.442 (the green short-dashed curves) and $H/|J| = 2.558$ and 2.562 (the green dash-dotted curves) from the corresponding two adjoining regions where three-peak structure in the behavior of the specific heat capacity is observed (see Fig. 7). In addition, the one-peak behavior of the specific heat capacity for parameters $H/|J| = 2.5$ and $\alpha = 0.5$ (the solid blue curve), where the neighboring zeroth-order ground state $g^{(2)}_{2,0}$ is formed, is included for comparison.

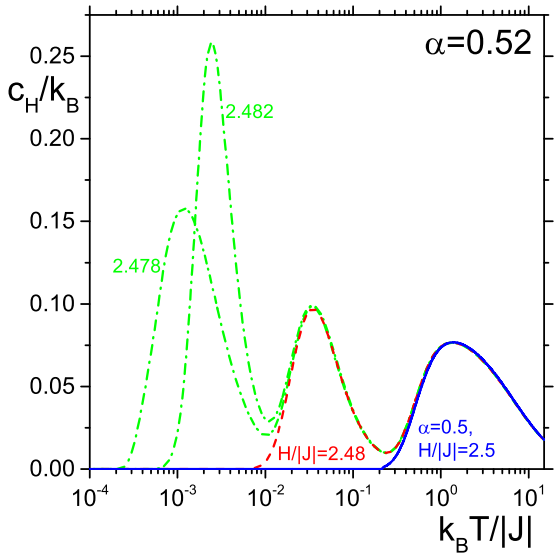

FIG. 10. The behavior of the specific heat capacity as a function of the reduced temperature for parameter $\alpha = 0.52$ and for three representative values of the external magnetic field chosen from three different neighboring regions of the parametric space where two and three peaks are formed, namely, for $H/|J| = 2.48$ (the red dashed curve) for which the specific heat capacity exhibits two-peak structure and for $H/|J| = 2.478$ and 2.482 (the green dash-dotted curves) from the corresponding left and right adjoining regions where three-peak structure in the behavior of the specific heat capacity is observed (see Fig. 7). In addition, again, the one-peak behavior of the specific heat capacity for parameters $H/|J| = 2.5$ and $\alpha = 0.5$ (the solid blue curve), where the neighboring zeroth-order ground state $g^{(2)}_{2,0}$ is formed, is included for comparison.

solid (blue) curves in Figs. 9–11 correspond to the one-peak behavior of the specific heat capacity directly at points, where the zeroth-order ground states $g^{(1)}_{2,0}$ and $g^{(2)}_{2,0}$, respectively, are realized. The existence of the two-peak behavior of the specific heat capacity on the corresponding segments of lines $\mathfrak{g}^{(1)}_{2,1}$, $\mathfrak{g}^{(3)}_{2,1}$, $\mathfrak{g}^{(4)}_{2,1}$, and $\mathfrak{g}^{(5)}_{2,1}$ (see Fig. 5–8), where the first-order ground states $g^{(1)}_{2,1}$, $g^{(3)}_{2,1}$, $g^{(4)}_{2,1}$, and $g^{(5)}_{2,1}$ are realized in the limit $T \to 0$, is demonstrated in Figs. 9–11 by the dashed (red) curves for given values of the external magnetic field. Finally, the dash-dotted as well as the short-dashed (green) curves in these figures demonstrate the typical three-peak structure in the temperature behavior of the specific heat capacity from the corresponding regions denoted by green Roman numeral III in Figs. 7 and 8.

As follows from Figs. 9–11, the peaks in the behavior of the specific heat capacity for parameters for which the zeroth-order ground states are realized (the solid blue curves) have the same properties (the same positions as well as heights) as the corresponding peaks in the behavior of the specific heat capacity for parameters of the model for which the neighboring ground states of higher orders are formed. At the same time, the same is valid for the second (Schottky-type) peaks in the behavior of the specific heat capacity described by the red dashed curves in Figs. 9–11, which have the same properties as the corresponding peaks in the behavior of the specific heat capacity for parameter values from subregions of $\mathcal{G}_{2,2}$, where the three-peak structure in the behavior of the specific heat capacity exists (the green dash-dotted and short-dashed curves).

This low-temperature behavior of the specific heat capacity is directly related to the cascade formation of the strict residual-entropy hierarchies of the neighboring ground states of all orders, as is demonstrated explicitly in Figs. 12–14, where the temperature behavior of the entropy is shown for the same model parameters as in Figs. 9–11.

On the other hand, the specific heat capacity as a function of the temperature demonstrates qualitatively different behavior in the vicinity of neighboring ground states of different orders, the strict residual-entropy hierarchy of which is violated. Such behavior is demonstrated explicitly in Fig. 15, where the temperature behavior of the specific heat capacity is shown for $\alpha = 1.02$ and for various values of the external magnetic field from the left and right vicinity of $H/|J| = 2$, for which the first-order ground state $g^{(2)}_{2,1}$ is realized when $\alpha > 1$. In addition, again the curve of the specific heat capacity for parameters for which the neighboring zeroth-order ground state $g^{(1)}_{2,0}$ is realized is shown for comparison (the blue solid curve in Fig. 15). Here, regardless of the value of the external magnetic field, the specific heat capacity exhibits at most the two-peak structure in its temperature behavior [see the dashed (red), short-dashed (green), and dash-dotted (dark yellow) curves]. Note that the dashed (red) curve corresponds to the parameters from line $\mathfrak{g}^{(2)}_{2,1}$ on which the first-order ground

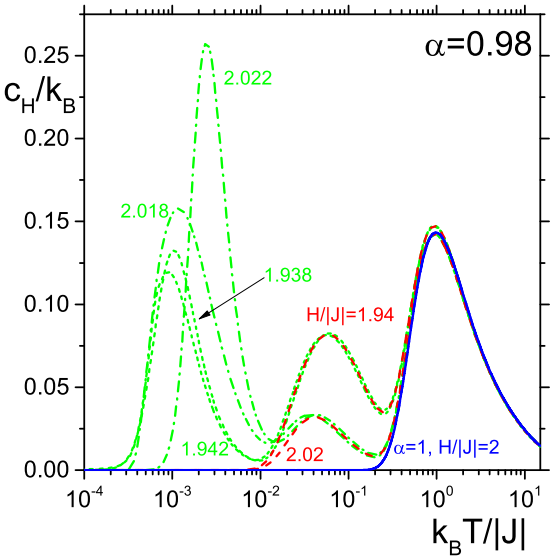

FIG. 11. The behavior of the specific heat capacity as a function of the reduced temperature for parameter $\alpha = 0.98$ and for six representative values of the external magnetic field chosen from six different regions of the parametric space where two and three peaks are formed, namely, for $H/|J| = 1.94$ and 2.02 (the red dashed curves) for which the specific heat capacity exhibits the two-peak structure and for $H/|J| = 1.938$ and 1.942 (the green short-dashed curves) and $H/|J| = 2.018$ and 2.022 (the green dash-dotted curves) from the corresponding two adjoining regions where the three-peak structure in the behavior of the specific heat capacity is observed (see Fig. 8). In addition, the one-peak behavior of the specific heat capacity for parameters $H/|J| = 2$ and $\alpha = 1$ (the solid blue curve), where the neighboring zeroth-order ground state $g^{(1)}_{2,0}$ is formed, is included for comparison.

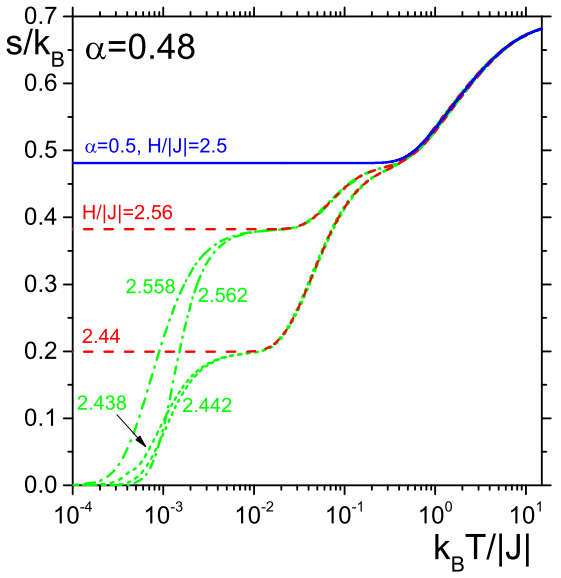

FIG. 12. The demonstration of the cascade temperature behavior of the entropy per site of the model for the same parameter values as in Fig. 9.

state $g^{(2)}_{2,1}$ is realized. On the other hand, the short-dashed (green) and dash-dotted (dark yellow) curves correspond to the parameters from adjoining regions $\mathfrak{g}^{(1)}_{2,2}$ and $\mathfrak{g}^{(2)}_{2,2}$ in which the corresponding second-order ground states $g^{(1)}_{2,2}$ and $g^{(2)}_{2,2}$ are formed in the limit $T \to 0$. However, due to the fact that the strict hierarchy between these neighboring ground states of different orders is violated, the third peak in the behavior of the specific heat capacity is not present here. Moreover, as is also evident from Fig. 15, the positions as well as heights of the Schottky-type peaks, i.e., the additional peak to the standard peak of the specific heat capacity that is formed at lower temperatures, are different for model parameters from the left and right vicinity of the line $\mathfrak{g}^{(2)}_{2,1}$, where the first-order ground state $g^{(2)}_{2,1}$ is formed. However, these peaks become very similar when the magnetic fields from the left and right simultaneously tend to $H/|J| = 2$ (see the corresponding couples of curves for $H/|J| = 1.998$ and 2.002 and $H/|J| = 1.9998$ and 2.0002). At the same time, they approach the curve of the specific heat capacity for $H/|J| = 2$ [the dashed (red) curve in Fig. 15].

This behavior of the specific heat capacity in the vicinity of the line $\mathfrak{g}^{(2)}_{2,1}$, where the first-order ground state $g^{(2)}_{2,1}$ is formed in the zero-temperature limit, is directly related to the nonexistence of the strict residual-entropy hierarchies among ground states of all different orders (see Fig. 4). As is explicitly evident from Fig. 16, the absence of the strict residual-entropy hierarchy between the first-order ground state $g^{(2)}_{2,1}$ and the second-order ground states $g^{(1)}_{2,2}$ and $g^{(2)}_{2,2}$ leads to the reduction of the three-level cascade temperature behavior of the entropy (see Figs. 12–14), which must exist when the hierarchy is strict, to the two-level one.

Thus, the presence of a strong enough ($|\alpha| > 1$) multisite interaction within elementary triangles in the framework of the antiferromagnetic model on the zigzag ladder not only reduces the number of different ground states of the model but also leads to the violation of the strict residual-entropy

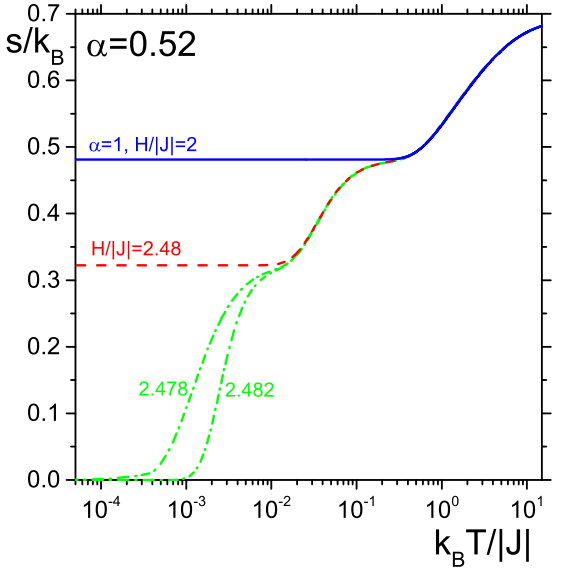

FIG. 13. The demonstration of the cascade temperature behavior of the entropy per site of the model for the same parameter values as in Fig. 10.

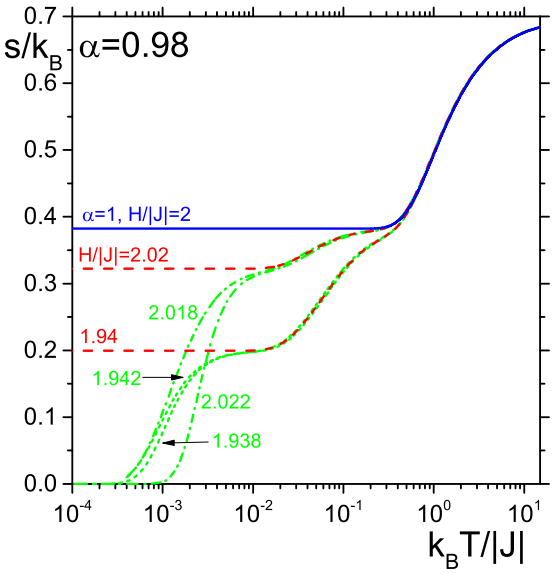

FIG. 14. The demonstration of the cascade temperature behavior of the entropy per site of the model for the same parameter values as in Fig. 11.

hierarchies and, as a result, to qualitatively different temperature behavior of the specific heat capacity. Moreover, as is discussed below, the violation of the strict residual-entropy hierarchy among neighboring ground states has also nontrivial

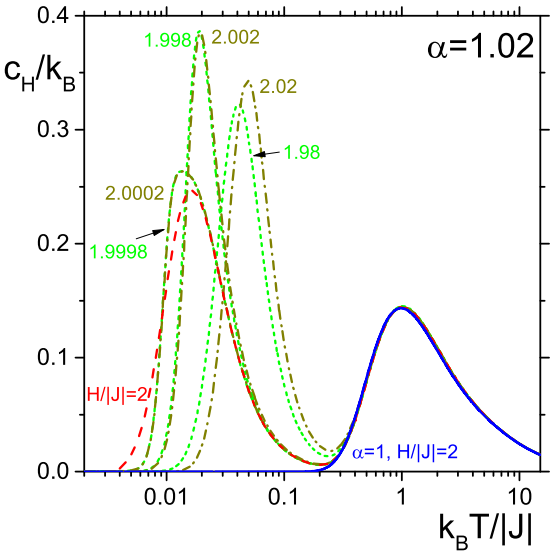

FIG. 15. The behavior of the specific heat capacity as a function of the reduced temperature for parameter $\alpha = 1.02$ and for various values of the external magnetic field in the vicinity of $H/|J| = 2$ where two peaks in the behavior of the specific heat capacity are formed, namely, directly for $H/|J| = 2$ (the red dashed curve), for which the first-order ground state $g^{(2)}_{2,1}$ is formed in zero-temperature limit, and for representative values of the external magnetic field from its left vicinity, namely, for $H/|J| = 1.98$, 1.998, and 1.9998 (the green short-dashed curves), as well as from its right vicinity for $H/|J| = 2.02$, 2.002, and 2.0002 (the dark-yellow dash-dotted curves). In addition, the one-peak behavior of the specific heat capacity for parameters $H/|J| = 2$ and $\alpha = 1$ (the solid blue curve), where the neighboring zeroth-order ground state $g^{(1)}_{2,0}$ is formed, is included for comparison.

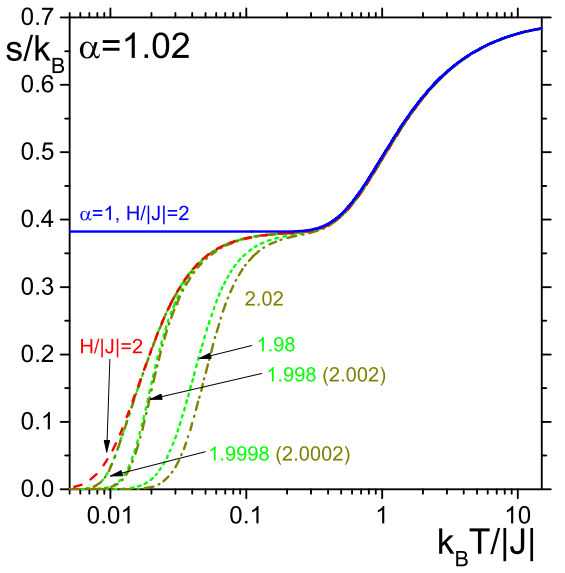

FIG. 16. The demonstration of the reduced two-level cascade temperature behavior of the entropy per site of the model for the same parameter values as in Fig. 15.

consequences for the behavior of the specific heat capacity as a function of the external magnetic field.

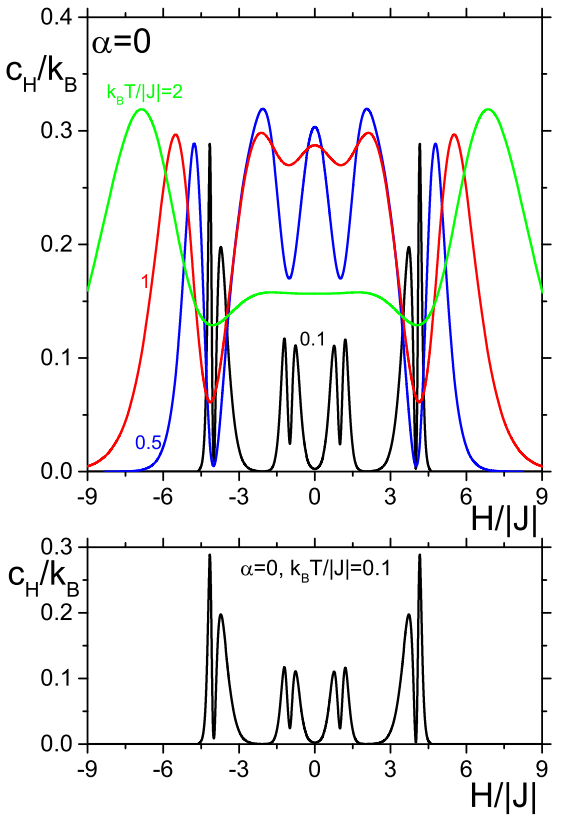

FIG. 17. Upper panel: The dependence of the specific heat capacity as a function of the external magnetic field for various values of the reduced temperature and for the parameter $\alpha = 0$. Lower panel: The explicit illustration of the field-induced sharp double-peak structure in the low-temperature behavior of the specific heat capacity for $k_BT/|J| = 0.1$.

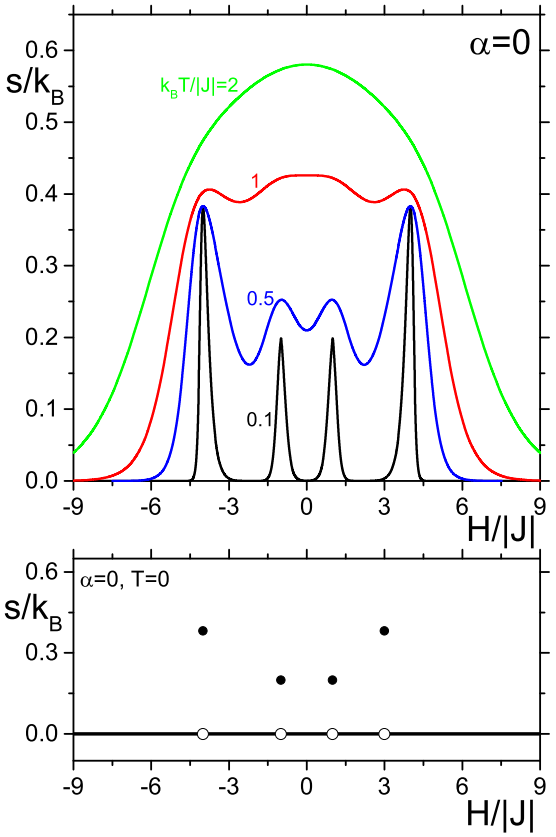

FIG. 18. Upper panel: The dependence of the entropy per site of the model as a function of the external magnetic field for the same parameter values as in Fig. 17. Lower panel: The entropy of the model as a function of the external magnetic field at the zero temperature for $\alpha = 0$.

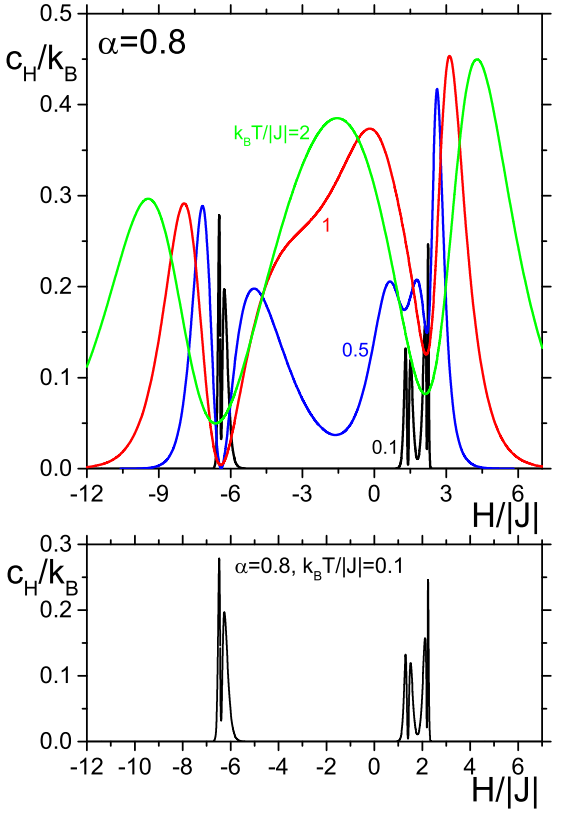

FIG. 19. Upper panel: The dependence of the specific heat capacity as a function of the external magnetic field for various values of the reduced temperature and for the parameter $\alpha = 0.8$. Lower panel: The explicit illustration of the field-induced sharp double-peak structure in the low-temperature behavior of the specific heat capacity for $k_BT/|J| = 0.1$.

Again, when the residual-entropy hierarchy among neighboring ground states of all orders is strict then one observes a typical low-temperature behavior of the specific heat capacity as a function of the external magnetic field. First of all, in the upper panel of Fig. 17, the behavior of the specific heat capacity as a function of the external magnetic field is shown for several values of the temperature for the case without the multisite interaction, i.e., for $\alpha = 0$. Here, in accordance with the detailed discussion present in Ref. [38], one can see the formation of a typical field-induced sharp double-peak structure at low temperatures centered in the magnetic field absolute values $|H/J| = 1$ and 4, for which the corresponding highly macroscopically degenerated single-point ground states are formed in the limit $T \to 0$. This can be seen explicitly in the lower panel of Fig. 17, where the curve for $k_BT/|J| = 0.1$ is shown once more for clarity. At the same time, the corresponding formation of the residual entropies of the single-point ground states as a function of the external magnetic field is shown in the upper panel of Fig. 18. The residual entropies of the model for the case $\alpha = 0$ are demonstrated in the lower panel of Fig. 18.

Qualitatively similar behavior of the specific heat capacity as a function of the external magnetic field (with formation of the sharp double-peak structure around each value of the external magnetic field, for which the single-point ground states are formed) is also observed in the model with the presence of the multisite interaction when its strength is weaker or at most equal to the nearest-neighbor antiferromagnetic interaction, i.e., when $|\alpha| \leqslant 1$. The influence of the multisite interaction on the behavior of the specific heat capacity as a function of the external magnetic field is demonstrated in Fig. 19 for $\alpha = 0.8$. One can see that, in this case, the presence of the multisite interaction leads to the reduction of the system of the ground states of the model but, due to the fact that all residual-entropy hierarchies among neighboring ground states are strict, the low-temperature formation of the double-peak structure in the specific heat capacity is again present (see the lower panel of Fig. 19). The only difference is the reduced number of formed double peaks related to the reduced number of different ground states. The corresponding behavior of the entropy of the model as a function of the external magnetic field for $\alpha = 0.8$ and for various values of the temperature is shown in the upper panel of Fig. 20. The formation of the residual entropies of all single-point ground states is evident from this figure, which are shown explicitly in the lower panel of Fig. 20.

However, qualitatively different behavior of the specific heat capacity as a function of the external magnetic field is observed when $|\alpha| > 1$. In this situation, as follows from Figs. 2 and 3, except of the saturated plateau-like ground

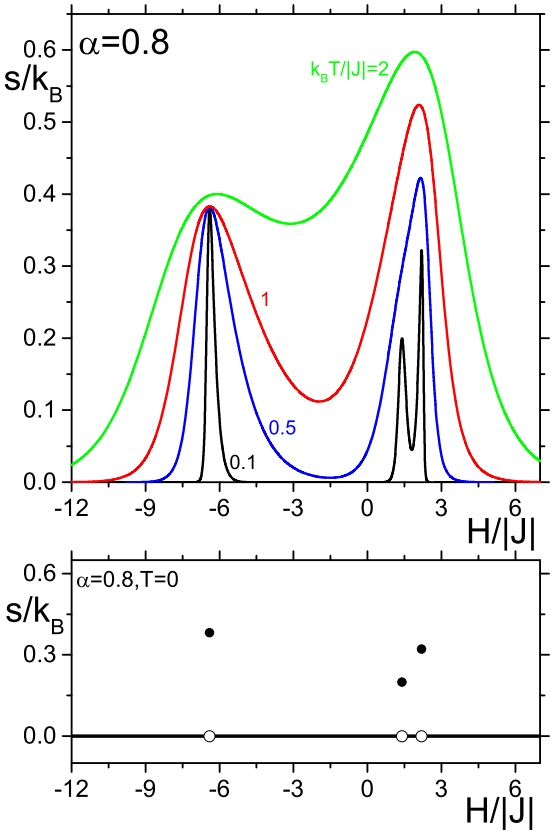

FIG. 20. Upper panel: The dependence of the entropy per site of the model as a function of the external magnetic field for the same parameter values as in Fig. 17. Lower panel: The entropy of the model as a function of the external magnetic field at the zero temperature for $\alpha = 0.8$.

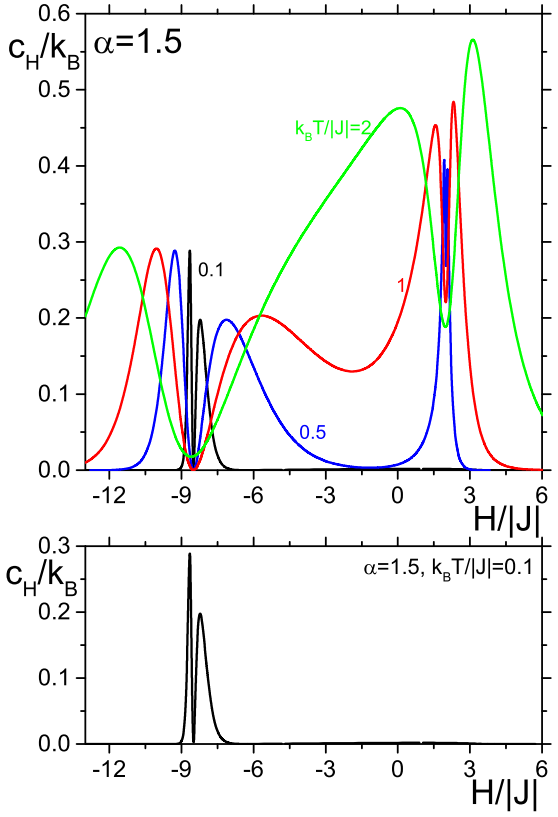

FIG. 21. Upper panel: The dependence of the specific heat capacity as a function of the external magnetic field for various values of the reduced temperature and for the parameter $\alpha = 1.5$. Lower panel: The explicit illustration of the field-induced sharp double-peak structure in the low-temperature behavior of the specific heat capacity for $k_BT/|J| = 0.1$.

states, the system exhibits only one plateau ground state with $|m| = 1/3$ and two single-point ground states of the first order that separate them (the solid and dotted lines in Fig. 2). But, as was discussed in the previous section, while, in this case, the magnetization properties of all neighboring ground states are different, the second-order ground states $g^{(1)}_{2,2}$ and $g^{(2)}_{2,2}$ as well as $g^{(4)}_{2,2}$ and $g^{(5)}_{2,2}$ are separated by the first-order ground state $g^{(2)}_{2,1}$ and $g^{(6)}_{2,1}$, respectively, the entropy of which is the same (equal to zero); i.e., the strict entropy hierarchy among them is violated. This fact has nontrivial impact on the behavior of the specific heat capacity as a function of the external magnetic field, which is demonstrated in detail in Figs. 21–24.

In Fig. 21, the specific heat capacity as a function of the external magnetic field for various values of temperatures is shown for $\alpha = 1.5$. For this value of the parameter α, the model exhibits the existence of two first-order single-point ground states $g^{(2)}_{2,1}$ and $g^{(8)}_{2,1}$, which are formed for $H/|J| = 2$ and -8.5, respectively. This fact is again visible in the behavior of the specific heat capacity shown in the upper panel of Fig. 21. But, while the behavior of the specific heat capacity in the vicinity of the magnetic field value $H/|J| = -8.5$ is completely the same as was already discussed above for $|\alpha| < 1$ (with the formation of the typical field-induced sharp double-peak structure for low temperatures centered directly at this value of the magnetic field), the behavior of the specific heat capacity in the vicinity of the magnetic field $H/|J| = 2$ is considerably different and no double-peak structure exists for low temperatures in this case. This is demonstrated in the lower panel of Fig. 21 for the reduced temperature $k_BT/|J| = 0.1$. This difference in the behavior of the specific heat capacity is directly related to the corresponding difference in the entropy behavior as a function of the external magnetic field shown explicitly in the upper panel of Fig. 22, where it is shown that while the entropy obtains its nonzero residual value in the zero-temperature limit for $H/|J| = -8.5$, the entropy tends to zero in this limit for $H/|J| = 2$ (see the lower panel of Fig. 22).

It is also instructive to compare in detail the low-temperature properties of the specific heat capacity as a function of the external magnetic field in the vicinity of these two specific values of the magnetic field. As follows from Fig. 23, in the case, when the entropy hierarchy among neighboring different-order ground states is strict, the double-peak structure in the behavior of the specific heat capacity is formed in the vicinity of the corresponding value of the magnetic field for relatively large values of temperature. In this case, the behavior of the specific heat capacity remains qualitatively the same when the temperature decreases and, at the same time, the formed double-peak structure becomes sharper and more pronounced. On

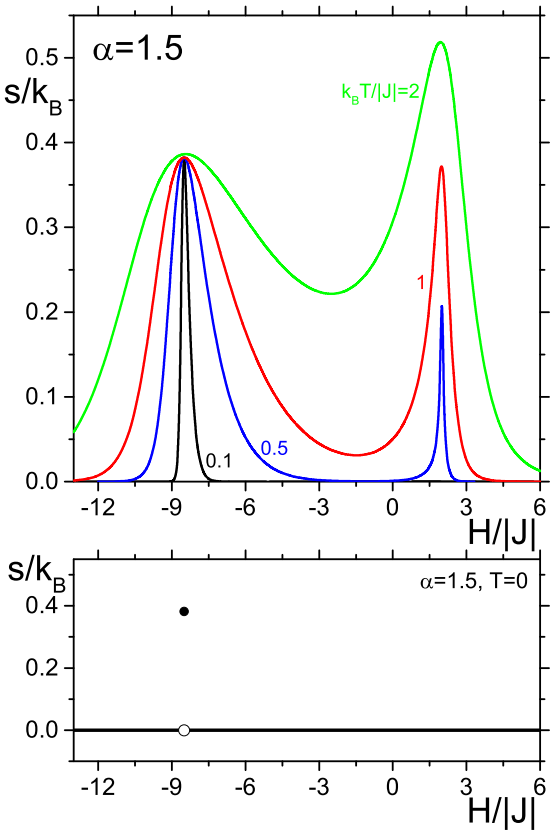

FIG. 22. Upper panel: The dependence of the entropy per site of the model as a function of the external magnetic field for the same parameter values as in Fig. 17. Lower panel: The entropy of the model as a function of the external magnetic field at the zero temperature for $\alpha = 0.8$.

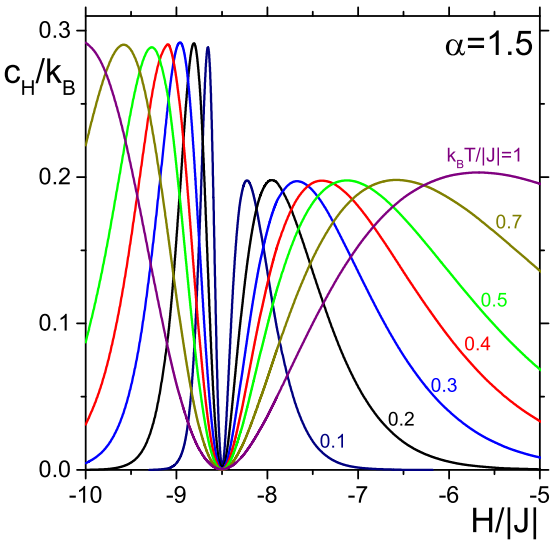

FIG. 23. Detailed illustration of the formation of the field-induced sharp double-peak structure in the low-temperature behavior of the specific heat capacity centered in the external magnetic value $H/|J| = -8.5$, for which the highly macroscopically degenerated single-point ground state is formed in the case $\alpha = 1.5$.

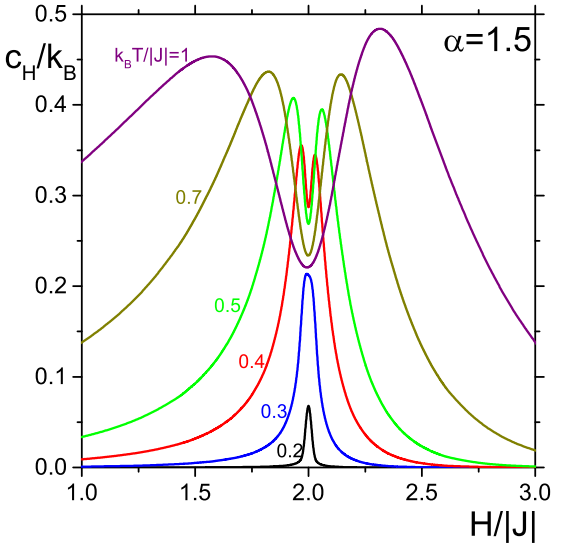

FIG. 24. Detailed illustration of the low-temperature behavior of the specific heat capacity for $\alpha = 1.5$ in the vicinity of the magnetic field value $H/|J| = 2$ for which the single-point ground state is formed that has the same zero value of the entropy as the neighboring plateau-like ground states, i.e., in the case in which the residual-entropy hierarchies between neighboring ground states of different orders are violated.

the other hand, as follows from Fig. 24, the behavior of the specific heat capacity around the magnetic field value $H/|J| = 2$ (where the first-order ground state is formed with the same zero entropy as both adjoining second-order ground states have) also exhibits the tendency to form double-peak structure at relatively large temperatures. But this double-peak structure disappears at some finite temperature for which the specific heat capacity comes to exhibit the one-peak structure only that disappears continuously in the zero-temperature limit.

As follows from the above discussion, the low-temperature behavior of the specific heat capacity as a function of the external magnetic field is significantly different in the vicinity of the magnetic field values, for which single-point ground states are formed in the limit $T \to 0$ with higher values of the residual entropies than neighboring plateau-like ground states, than in the vicinity of the values of the magnetic field, where the single-point ground states are formed with the same entropy as the corresponding adjoining plateaus have. However, from the experimental point of view, the very existence and formation of different-order ground states in the system at some external magnetic field values can be directly detected in both these cases by the corresponding typical behavior of the specific heat capacity described above.

V. CONCLUSION

In conclusion, let us summarize briefly the main results obtained in this paper.

In the present paper, we have investigated in detail thermodynamical consequences of the hierarchy violation between residual entropies of neighboring ground states of different orders in the framework of the exactly solvable antiferromag-

netic Ising model with the presence of multisite interaction in the external magnetic field on the geometrically frustrated zigzag ladder.

First of all, a unique classification of the set of all ground states of the model is performed from the point of view of their dimensionality (i.e., from the point of view of the spatial dimension of the region in the ground-state parametric space, in which the corresponding ground state is realized) and their residual entropies are exactly determined. It is shown that the ground-state picture of the model from the magnetization point of view is different than that from the entropy point of view, namely, that there exist the ground states of lower-order (the first-order ground states) whose residual entropy is the same as the entropies of the neighboring higher-order ground states (the second-order ground states), although all of them have different values of magnetization. This means that the entropy hierarchies between neighboring ground states of different orders are violated in this case.

Further, it is shown in detail that this residual-entropy hierarchy violation has nontrivial consequences on the behavior of the specific heat capacity as a function of the temperature as well as of the external magnetic field. On one hand, it is shown that the absence of the strict hierarchy between residual entropies of the neighboring ground states of different orders leads to the reduction of the possible number of peaks in the low-temperature behavior of the specific heat capacity in the corresponding regions of the ground-state parametric space. On the other hand, the violation of this strict entropy hierarchy also leads to qualitatively significantly different behavior of the specific heat capacity as a function of the external magnetic field that can be directly measured by experiments. Namely, while, in the cases when the hierarchies between residual entropies of neighboring ground states of different orders are strict, the specific heat capacity as a function of the external magnetic field exhibits the formation of typical field-induced sharp double-peak structures centered in the magnetic field values for which the corresponding single-point ground states are formed in the limit $T \to 0$ (see Fig. 23), in the case in which this hierarchy is violated, the specific heat capacity as a function of the external magnetic field also exhibits the tendency to form double-peak structure at relatively large temperatures but this double-peak structure disappears at some finite temperature and, subsequently, the remaining one-peak structure disappears continuously in the zero-temperature limit (see Fig. 24).

We suppose that the obtained theoretical results can be used in experiments for obtaining nontrivial information about macroscopic degeneracies of ground states of various frustrated magnetic materials. Namely, measuring the properties of the specific heat capacity as a function of the external magnetic field at low temperatures, one can not only identify the exact positions of all single-point ground states but also identify relations between their residual entropies and the residual entropies of the neighboring plateau-like ground states.

ACKNOWLEDGMENTS

The work was supported by VEGA Grants No. 2/0065/17 and No. 2/0058/19 of the Slovak Academy of Sciences, by Grant No. APVV-17-0020, and by the realization of the project ITMS No. 26220120029, based on the supporting operational Research and Development Program financed from the European Regional Development Fund.

[1] A. P. Ramirez, Annu. Rev. Mater. Sci. **24**, 453 (1994).
[2] N. P. Raju, E. Gmelin, and R. K. Kremer, Phys. Rev. B **46**, 5405 (1992).
[3] K. Ishida, M. Morishita, K. Yawata, and H. Fukuyama, Phys. Rev. Lett. **79**, 3451 (1997).
[4] V. K. Pecharsky and K. A. Gschneidner, Jr., Phys. Rev. Lett. **78**, 4494 (1997).
[5] M. J. Harris, S. T. Bramwell, P. C. W. Holdsworth, and J. D. M. Champion, Phys. Rev. Lett. **81**, 4496 (1998).
[6] B. Revaz, A. Junod, and A. Erb, Phys. Rev. B **58**, 11153 (1998).
[7] N. P. Raju, M. Dion, M. J. P. Gingras, T. E. Mason, and J. E. Greedan, Phys. Rev. B **59**, 14489 (1999).
[8] R. Siddharthan, B. S. Shastry, A. P. Ramirez, A. Hayashi, R. J. Cava, and S. Rosenkranz, Phys. Rev. Lett. **83**, 1854 (1999).
[9] A. P. Ramirez, A. Hayashi, R. J. Cava, R. Siddharthan, and B. S. Shastry, Nature (London) **399**, 333 (1999).
[10] R. G. Melko, B. C. den Hertog, and M. J. P. Gingras, Phys. Rev. Lett. **87**, 067203 (2001).
[11] K. Matsuhira, Z. Hiroi, T. Tayama, S. Takagi, and T. Sakakibara, J. Phys.: Condens. Matter **14**, L559 (2002).
[12] Z. Hiroi, K. Matsuhira, S. Takagi, T. Tayama, and T. Sakakibara, J. Phys. Soc. Jpn. **72**, 411 (2003).
[13] Z. Hiroi, K. Matsuhira, and M. Ogata, J. Phys. Soc. Jpn. **72**, 3045 (2003).
[14] S. Noguchi, T. Sakon, H. Nojiri, and M. Motokawa, Physica B **346-347**, 179 (2004).
[15] S. Noguchi, T. Sakon, H. Nojiri, and M. Motokawa, Physica B **346-347**, 183 (2004).
[16] S. S. Sosin, L. A. Prozorova, A. I. Smirnov, A. I. Golov, I. B. Berkutov, O. A. Petrenko, G. Balakrishnan, and M. E. Zhitomirsky, Phys. Rev. B **71**, 094413 (2005).
[17] L. Gondek, A. Szytula, D. Kaczorowski, A. Szewczyk, M. Gutowska, and P. Piekarz, J. Phys.: Condens. Matter **19**, 246225 (2007).
[18] X. Ke, M. L. Dahlberg, E. Morosan, J. A. Fleitman, R. J. Cava, and P. Schiffer, Phys. Rev. B **78**, 104411 (2008).
[19] P. Schobinger-Papamantellos, J. Rodríguez-Carvajal, L. D. Tung, C. Ritter, and K. H. J. Buschow, J. Phys.: Condens. Matter **20**, 195201 (2008).
[20] X. Ke, D. V. West, R. J. Cava, and P. Schiffer, Phys. Rev. B **80**, 144426 (2009).
[21] J. S. Gardner, M. J. P. Gingras, and J. E. Greedan, Rev. Mod. Phys. **82**, 53 (2010).
[22] D. O'Flynn, M. R. Lees, and G. Balakrishnan, J. Phys.: Condens. Matter **26**, 256002 (2014).
[23] I. Panneer Muthuselvam, R. Sankar, A. V. Ushakov, W. T. Chen, G. Narsinga Rao, S. V. Streltsov, S. K. Karna, L. Zhao, M.-K. Wu, and F. C. Chou, J. Phys.: Condens. Matter **27**, 456001 (2015).

[24] S. Pakhira, C. Mazumdar, R. Ranganathan, S. Giri, and M. Avdeev, Phys. Rev. B **94**, 104414 (2016).
[25] D. Villundas, T. Tsutaoka, and J. M. Hernàndes Ferràs, J. Magn. Magn. Mater. **405**, 282 (2016).
[26] E. V. Shevchenko, E. V. Charnaya, M. K. Lee, L. J. Chang, E. N. Khazanov, A. V. Taranov, and A. S. Bugaev, Phys. Lett. A **381**, 330 (2017).
[27] J. Brambleby, P. A. Goddard, J. Singleton, M. Jaime, T. Lancaster, L. Huang, J. Wosnitza, C. V. Topping, K. E. Carreiro, H. E. Tran, Z. E. Manson, and J. L. Manson, Phys. Rev. B **95**, 024404 (2017).
[28] S. Lucas, K. Grube, C.-H. Huang, A. Sakai, W. Wunderlich, E. L. Green, J. Wosnitza, V. Fritsch, P. Gegenwart, O. Stockert, and H. v. Löhneysen, Phys. Rev. Lett. **118**, 107204 (2017).
[29] M. Ito, T. Furuta, K. Kai, A. Taira, K. Onda, I. Shigeta, and M. Hiroi, J. Magn. Magn. Mater. **428**, 390 (2017).
[30] E. Jurčišinová and M. Jurčišin, Phys. Rev. E **97**, 052129 (2018).
[31] M. D. Kuzmin and A. M. Tishin, J. Phys. D **24**, 2039 (1991).
[32] M. E. Zhitomirsky, Phys. Rev. B **67**, 104421 (2003).
[33] K. A. Gschneidner, V. K. Pecharsky, and A. O. Tsokol, Rep. Prog. Phys. **68**, 1479 (2005).
[34] A. M. Tishin, Y. I. Spichkin, V. I. Zverev, and P. W. Egolf, Int. J. Refrig. **68**, 177 (2016).
[35] B. Wolf, U. Tutsch, S. Dörschung, C. Krellner, F. Ritter, W. Assmus, and M. Lang, J. Appl. Phys. **120**, 142112 (2016).
[36] E. Jurčišinová and M. Jurčišin, Phys. Rev. E **96**, 052128 (2017).
[37] M. Orendač, S. Gabáni, E. Gažo, G. Pristaš, N. Shitsevalova, K. Siemensmeyer, and K. Flachbart, Sci. Rep. **8**, 10933 (2018).
[38] E. Jurčišinová and M. Jurčišin, J. Magn. Magn. Mater. **451**, 137 (2018).
[39] E. Jurčišinová and M. Jurčišin, Phys. Rev. E **90**, 032108 (2014).
[40] Z. N. C. Ha, Phys. Rev. B **59**, 1559 (1999).
[41] N. Maeshima and K. Okunishi, Phys. Rev. B **62**, 934 (2000).
[42] D. C. Cabra, A. Honecker, and P. Pujol, Eur. Phys. J. B **13**, 55 (2000).
[43] K. Okunishi and N. Maeshima, Phys. Rev. B **64**, 212406 (2001).
[44] F. A. Kassan-ongly, Phase Transitions **74**, 353 (2001).
[45] J. Schulenburg, A. Honecker, J. Schnack, J. Richter, and H.-J. Schmidt, Phys. Rev. Lett. **88**, 167207 (2002).
[46] I. Bose and E. Chattopadhyay, Phys. Rev. A **66**, 062320 (2002).
[47] M. T. Batchelor, X.-W. Guan, N. Oelkers, K. Sakai, Z. Tsuboi, and A. Foerster, Phys. Rev. Lett. **91**, 217202 (2003).
[48] A. Tokuno, K. Okamoto, and T. Tonegawa, Prog. Theor. Phys. Suppl. **159**, 265 (2005).
[49] H. T. Lu, Y. J. Wang, Shaojin Qin, and T. Xiang, Phys. Rev. B **74**, 134425 (2006).
[50] D. V. Dmitriev and V. Ya. Krivnov, Phys. Rev. B **77**, 024401 (2008).
[51] D. N. Sheng, O. I. Motrunich, and M. P. A. Fisher, Phys. Rev. B **79**, 205112 (2009).
[52] T. Hikihara, T. Momoi, A. Furusaki, and H. Kawamura, Phys. Rev. B **81**, 224433 (2010).
[53] S. Furukawa, M. Sato, S. Onoda, and A. Furusaki, Phys. Rev. B **86**, 094417 (2012).
[54] I. T. Shyiko, I. P. McCulloch, J. V. Gumenjuk-Sichevska, and A. K. Kolezhuk, Phys. Rev. B **88**, 014403 (2013).
[55] J. Strečka, O. Rojas, T. Verkholyak, and M. L. Lyra, Phys. Rev. E **89**, 022143 (2014).
[56] B. Grenier, S. Petit, V. Simonet, E. Canévet, L.-P. Regnault, S. Raymond, B. Canals, C. Berthier, and P. Lejay, Phys. Rev. Lett. **114**, 017201 (2015).
[57] A. Parvej and M. Kumar, J. Magn. Magn. Mater. **401**, 96 (2016).
[58] M. Pregelj, O. Zaharko, U. Stuhr, A. Zorko, H. Berger, A. Prokofiev, and D. Arčon, Phys. Rev. B **98**, 094405 (2018).
[59] M. Matsuda and K. Katsumata, J. Magn. Magn. Mater. **140–144**, 1671 (1995).
[60] M. Matsuda, K. Katsumata, K. M. Kojima, M. Larkin, G. M. Luke, J. Merrin, B. Nachumi, Y. J. Uemura, H. Eisaki, N. Motoyama, S. Uchida, and G. Shirane, Phys. Rev. B **55**, R11953 (1997).
[61] M. Azuma, Z. Hiroi, M. Takano, K. Ishida, and Y. Kitaoka, Phys. Rev. Lett. **73**, 3463 (1994).
[62] T. Imai, K. R. Thurber, K. M. Shen, A. W. Hunt, and F. C. Chou, Phys. Rev. Lett. **81**, 220 (1998).
[63] Y. Mizuno, T. Tohyama, S. Maekawa, T. Osafune, N. Motoyama, H. Eisaki, and S. Uchida, Phys. Rev. B **57**, 5326 (1998).
[64] G. Chaboussant, P. A. Crowell, L. P. Lévy, O. Piovesana, A. Madouri, and D. Mailly, Phys. Rev. B **55**, 3046 (1997).
[65] W. Shiramura, K. Takatsu, H. Tanaka, K. Kamishina, M. Takahashi, H. Mitamura, and T. Goto, J. Phys. Soc. Jpn. **66**, 1900 (1997).
[66] W. Shiramura *et al.*, J. Phys. Soc. Jpn. **67**, 1548 (1998).
[67] S.-L. Drechsler, N. Tristan, R. Klingeler, B. Büchner, J. Richter, J. Malek, O. Volkova, A. Vasiliev, M. Schmitt, A. Ormeci, C. Loison, W. Schnelle, and H. Rosner, J. Phys.: Condens. Matter **19**, 145230 (2007).
[68] A. Mohan, S. Singh, S. Partzsch, M. Zwiebler, J. Geck, S. Wurmehl, B. Büchner, and C. Hess, J. Cryst. Growth **448**, 21 (2016).
[69] I. L. Danilovich, E. V. Karpova, I. V. Morozov, A. V. Ushakov, S. V. Streltsov, A. A. Shakin, O. S. Volkova, E. A. Zvereva, and A. N. Vasiliev, Chem. Phys. Chem. **18**, 2482 (2017).
[70] K. T. Lai and M. Valldor, Sci. Rep. **7**, 43767 (2017).